Recording Quality Is Systematically Related to Electrode Impedance

ADVANCED HEALTHCARE MATERIALS
www.advhealthmat.de

Recording Quality Is Systematically Related to Electrode Impedance

*Christopher M. Lewis, Christian Boehler, Rickard Liljemalm, Pascal Fries, Thomas Stieglitz, and Maria Asplund**

Extracellular recordings with planar microelectrodes are the gold standard technique for recording the fast action potentials of neurons in the intact brain. The introduction of microfabrication techniques has revolutionized the in vivo recording of neuronal activity and introduced high-density, multi-electrode arrays that increase the spatial resolution of recordings and the number of neurons that can be simultaneously recorded. Despite these innovations, there is still debate about the ideal electrical transfer characteristics of extracellular electrodes. This uncertainty is partly due to the lack of systematic studies comparing electrodes with different characteristics, particularly for chronically implanted arrays over extended time periods. Here a high-density, flexible, and thin-film array is fabricated and tested, containing four distinct electrode types differing in surface material and surface topology and, thus, impedance. It is found that recording quality is strongly related to electrode impedance with signal amplitude and unit yield negatively correlated to impedance. Electrode impedances are stable for the duration of the experiment (up to 12 weeks) and recording quality does not deteriorate. The findings support the expectation from the theory that recording quality will increase as impedance decreases.

1. Introduction

Microelectrodes are essential tools within neuroscience as they enable selective recording down to single-neuron resolution with single-spike precision.[1] In particular, the development of microelectrode arrays has revolutionized the possibilities of studying the brain in action, as the combined signal recorded on several closely spaced electrodes allows the signature of individual units to be distinguished from the complex mixture of nearby neurons.[2] Recordings made by electrodes considerably larger than a single neuron reflect a signal averaged from that larger area, whereas the spatially confined nature of a microelectrode results in a cleaner signature of the closest neurons, increasing the selectivity of the recording and the quality of the data obtained (**Figure 1**). Indeed, the ideal electrode would have minimal size and impedance to record the maximally localized and least attenuated signal. While such electrodes were difficult to construct with classical methods in which electrode size correlated negatively with impedance, modern fabrication and electrode coatings make it possible to approach this ideal.[2c,3]

Based on these considerations, the importance of reducing the contact size of electrodes is clear: it enables both improved spatial resolution and increased electrode density, which are crucial steps towards improving experimental access to brain activity. Moreover, reduced electrode sizes allow the overall size of an implant to be reduced for a given number of electrodes, minimizing tissue displacement, improving tissue integration and long-term recording quality.[3a,4] On the other hand, reducing electrode size results in increased electrochemical impedance which is expected to reduce the signal-to-

C. M. Lewis
Brain Research Institute
University of Zurich
Zurich 8057, Switzerland

C. Boehler, R. Liljemalm, T. Stieglitz, M. Asplund
Department of Microsystems Engineering (IMTEK)
University of Freiburg
79110 Freiburg, Germany
E-mail: maria.asplund@chalmers.se

C. Boehler, T. Stieglitz, M. Asplund
BrainLinks-BrainTools Center
University of Freiburg
79110 Freiburg, Germany

P. Fries
Ernst Strüngmann Institute (ESI) for Neuroscience in Cooperation with
Max Planck Society
Deutschordenstraße 46, 60528 Frankfurt, Germany

P. Fries
Donders Institute for Brain
Cognition and Behaviour
Radboud University
Kapittelweg 29, 6525 EN, Nijmegen, Netherland

M. Asplund
Department of Microtechnology and Nanoscience
Chalmers University of Technology
Kemivägen 9, Gothenburg 41258, Sweden

The ORCID identification number(s) for the author(s) of this article can be found under https://doi.org/10.1002/adhm.202303401

DOI: 10.1002/adhm.202303401

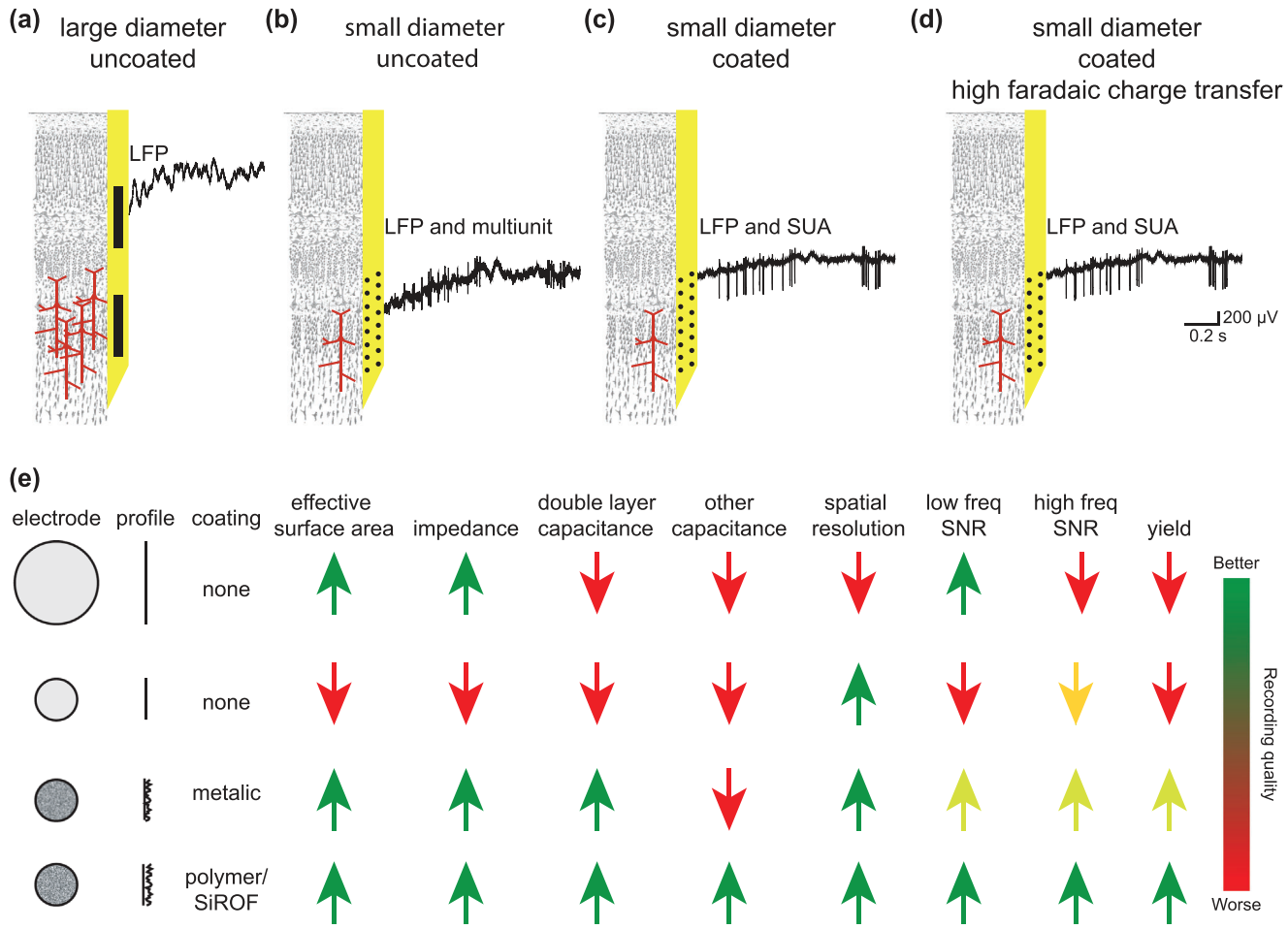

Figure 1. Electrode size and impedance affect recording characteristics. a) Large electrodes have low impedance, but their large size leads to spatial blurring, obscuring the source of high frequency action potentials and preventing the recording of single units. b) Small uncoated electrodes have high impedance and while they can record spatially localized signals, the reduction in signal often prevents the isolation of single units. c) Coating small electrodes increases the effective surface area and decrease the impedance, while maintaining the high spatial resolution, enabling isolation of single units. d) Coatings vary in their electrochemical properties that can further lower the effective impedance and increase the yield of single units and SNR. e) Electrode properties, such as their size and surface characteristics determine their effective surface area, and hence their impedance, capacitance, and the quality of the signal they can record. We used upwards arrows to indicate better recording quality and downward arrows to denote worse recording quality, while the saturation of the color denotes the relative position on this continuum (see color scale). Note that for impedance, upwards arrows correspond to lower impedance, which is beneficial for recording quality.

noise ratio (SNR), as the thermal noise will increase.[3d] According to theory, the electrode can be understood as an electrochemical impedance, which is dominated by capacitance, because electrons move freely in the electrode and recording system, while ions are the charge carriers in the brain. As a result, the electrode, in combination with the input impedance of the recording amplifier system acts as a high-pass filter on the recorded neurophysiological signals.[5] This may introduce phase shifts, as well as attenuate different components of the signal to different degrees. Over low to intermediate frequencies, the impedance of the typical electrode is orders of magnitude higher than in the high-frequency domain. In other words, the high-frequency signals experience the electrode "pass-band" while signals at lower frequencies experience its filtering characteristics.[6] Such effects are relevant in neuroscience because signals of interest may be significantly attenuated by common electrode materials when electrodes are made small enough to record spikes and they are not combined with low-impedance electrode coatings or a recording amplifier with significantly high input impedance.[5,6] It is helpful here to lend the engineering term "cut-off frequency" to describe the filtering properties of an electrode, defined as the frequency at which a signal magnitude is reduced by 3 dB with respect to the signal transfer in the pass-band. By reporting the cut-off frequency of the electrode, the neuroscientist user will know if the signals to be recorded are sufficiently high to be within the electrode pass band or, if they are in the frequency domain that will be attenuated in a frequency-dependent manner.[3d] For example, a platinum electrode with a diameter of 30 µm or less, has a cut-off frequency at 40 kHz or more, well above the biologically relevant range for neural recordings (Figure S1, Supporting Information). Thus, although such an electrode still may record signals, these will be influenced by the frequency-dependent

impedance characteristics, by phase shifts and significant attenuation.

To enable the benefits of a small electrode while maintaining a low impedance, electrode surfaces can be functionalized. Such functionalization can dramatically reduce electrode impedance and the attenuation of relevant signal components. Most surface functionalization approaches increase the electrode's effective surface area and capacitance by adding a three-dimensional structure to the two-dimensional surface, allowing the electrolytic contact area of the electrode to be much larger than its flat surface area.[3d] By simply adding roughness to the surface, it is possible to reduce the size of an electrode by several orders of magnitude, while maintaining the favorable impedance characteristics of the larger area (Figure 1). Some electrode coatings, in addition to their capacitive properties, add faradaic charge transfer qualities which may reduce impedance further, by providing additional signal transduction pathways between the electrode and the tissue. Examples of such materials are the conducting polymer-based electrode coatings like poly(3,4-ethylene dioxythiophene)-polystyrene sulphonate (PEDOT-PSS), and sputtered iridium oxide film (SIROF), materials with additional inherent mechanisms to absorb/expel charge which may act as a transducer between electrolytic and electronic signals. In short, more mechanisms can add further possibilities to facilitate signal transfer in parallel to the capacitive coupling.[7]

The development of low-impedance materials for neural microelectrodes is based on the theoretically well-grounded assumption that it will improve or maintain the quality of recorded data as electrodes are reduced in size. However, practical experience has been inconclusive and, in contrast to the expectation, has shown that microelectrodes with comparably high impedances are able to record single units.[1a,8] In fact, some studies have even suggested that the impedance of the electrode does not matter for the recording quality, an unexpected finding which is difficult to fully explain.[8] Such data suggest the theoretical conceptualization of an electrode as an impedance in a circuit with the tissue, might not represent the real-world situation of a recording microelectrode.[5] If true, this information would be of great significance, both to developers of microelectrode arrays and to the users of such technology, as this would imply that optimizing this aspect of the electrodes themselves is not necessary.

To shed light on whether impedance matters for the recording quality of implanted microelectrodes, we designed a series of experiments to approach this in two stages, first in vitro, simulating a recording situation in a beaker, and then in vivo, recording actual neural signals using implanted intracortical probes. Our two-stage experimental design was aimed at first analyzing the recording qualities of the electrodes in the absence of any biological variability, which would correspond to the typical environment during electrochemical characterization, such as impedance spectroscopy. Second, by taking the step to chronically implanted probes we were able to validate the in vitro findings in the biological setting. Electrodes with different materials, coatings, and surface topologies were placed side-by-side on the same substrate to ensure most similar boundary conditions during implantation and foreign body reaction after implantation.

In our study we chose to compare the performance of three different low-impedance electrode materials: a nanostructured platinum (nanoPt), PEDOT/PSS (here simply referred to as PEDOT) and SIROF against smooth thin-film platinum, all deposited onto electrodes of otherwise identical proportions.[9] The three materials were selected as they represent different types of low-impedance modifications, adding only roughness (nanoPt), in comparison to roughness and pseudocapacitive charge transfer in parallel (SIROF and PEDOT), as well as the additional benefit of an extremely hydrophilic surface provided by PEDOT. The latter has been reported to provide exceptional recording qualities, which would be expected based on the low electrochemical impedance but could also be enhanced by additional material properties improving the cell-surface interconnection.[10] The recording performance of the three candidate materials was compared among each other, to correlate their performances with their respective impedances, including identical electrodes of significantly higher impedance based on smooth platinum. In order to reduce the effect of biological variability as such, and during foreign body reaction succeeding implantation, we furthermore tailored flexible probes where these four electrode materials were intermingled on the same probe, at 45 µm pitch. Thus, each electrode would experience a similar signaling environment facilitating comparison and reducing the biological variability. Flexible micromachined substrates were chosen as a platform technology, as the reduction in scarring would contribute to more stable performance over time, thus making it more likely that the electrodes would be able to record from several viable neurons in parallel.[3a,11] This is worth noting as the added benefit of a low-impedance electrode may be influenced by the number of viable neurons available around the probe.

2. Results

2.1. Impedance Characteristics of Electrode Materials

Flexible polyimide-based thin-film probes were prepared according to previously published protocols, featuring micro-electrodes of equal size but with different electrode materials on their surfaces (**Figure 2**a-e).[3a] The electrode size was defined by a 5 µm deep trench etched into the top polyimide layer, exposing the electrode metal underneath, to ensure that all electrodes would have identical geometrical surface area regardless of which electrode material was added. Several different probe designs were fabricated, from implantable shanks with 12 µm diameter electrodes (outlined in detail in Figure S2, Supporting Information), to probes with electrodes of different sizes (shown in Figure S3, Supporting Information). In the latter case, the electrodes span the full range of diameters from 5 to 1000 µm. This allowed us to independently study the effect of reducing the impedance by increasing electrode area, and compare that to when an electrode coating was used to lower the impedance while the geometrical electrode area remained the same.

Four types of electrode materials were analyzed: smooth Pt, nanoPt, SIROF, and PEDOT/PSS. Pt was used as base metallization for every electrode, and the various electrode materials were coated onto the Pt according to established processes described elsewhere.[9,12] In the case of SIROF, this was deposited as part of the cleanroom wafer-level manufacturing process, using reactive sputtering. This results in a gradual transition from iridium to nanoporous iridium oxide, with an overall thickness of ≈700 nm. NanoPt and PEDOT/PSS are electrodeposited materials,

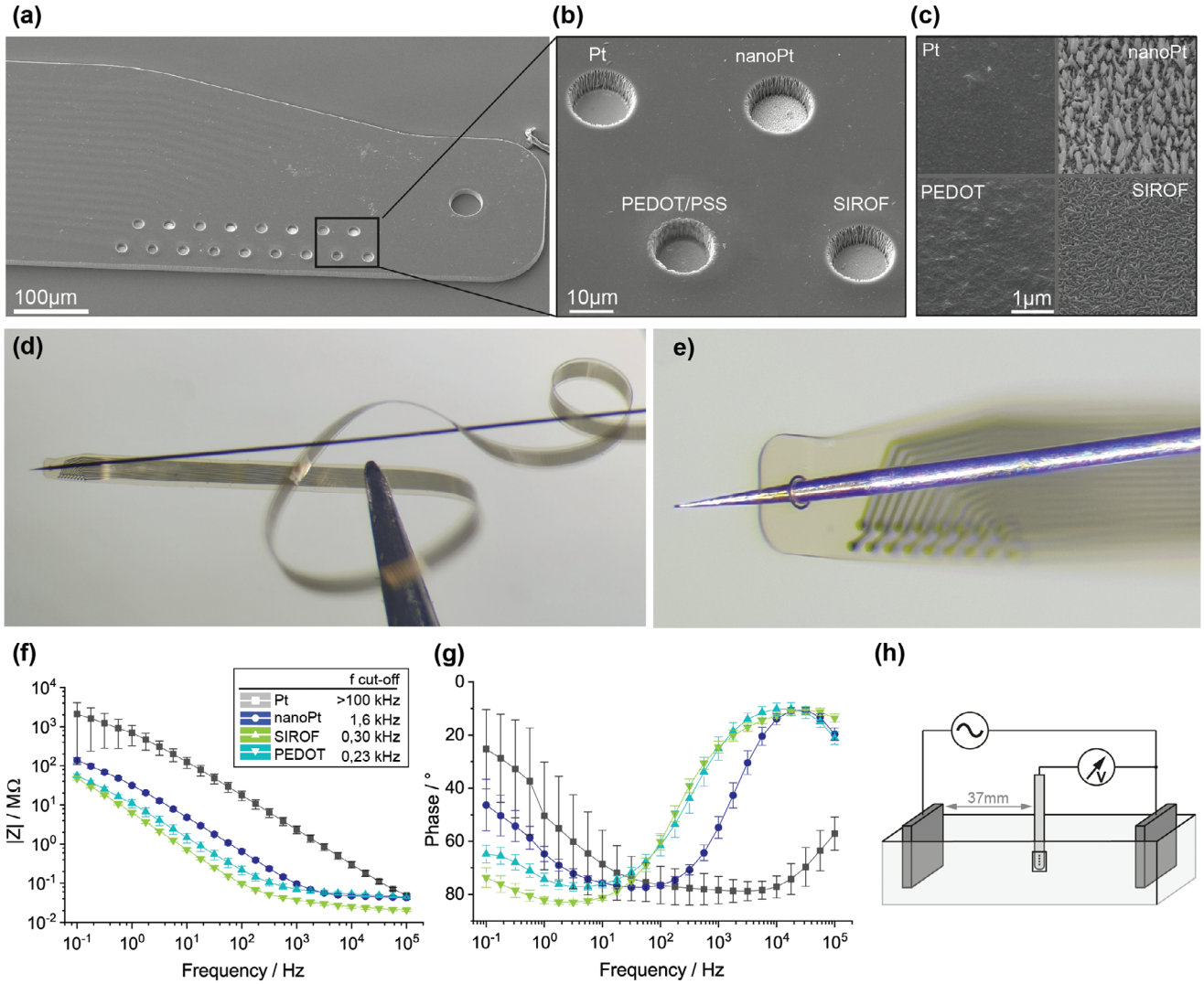

Figure 2. Flexible probe with different electrode coatings. a) Scanning Electron Microscopy (SEM) image of the probe showing the electrode configuration with 17 individual contact sites (12 µm diameter) arranged in a staggered pattern at the edge of the implant. b) Electrodes of different materials were intermingled on the probe so that all four materials were represented within an area of less than 60 × 60 µm2. c) The high-resolution SEM images of the electrode materials used within the same implant show distinct morphologies for each of the materials (Pt, nanoPt, SIROF, and PEDOT). d) The flexible probe where the central hole at the front serves for implanting the probe using a guide needle, here shown with a WTi tungsten rod (100 µm diameter) and with magnified view in (e), where the tip sharpening of the rod is visible. f) Impedance magnitude and g) phase angle based on EIS, averaged over 11 different probes, in total $n = 44$ sites per material (12 µm diameter), with standard deviation as error bars. Cut-off frequency as indicated in the inset is determined at a phase angle of 45°. h) Schematic illustration of the in vitro measurement setup for quantification of the SNR with the probe placed in the center between two lateral electrodes providing the test signal.

meaning these were added only after completion of all the cleanroom manufacturing steps. NanoPt was coated directly onto the bare Pt while PEDOT/PSS was coated on top of SIROF electrodes.[9b,12] As strong adhesion is achieved between SIROF and PEDOT/PSS, this ensures that the coating remains stably anchored to the base substrate throughout all experiments, including the chronic implantation over many months and the explanation thereafter. All coatings stay within the trench and do not exceed the surface of the substrate. It should be noted that the impedance characteristics of each electrode are dominated by the surface interaction, wherefore the underlying substrate (Pt or SIROF on Pt) will not influence performance other than stability.

For each individual electrode, the electrochemical impedance spectrum was measured from 0.1 Hz to 100 kHz, as summarized in the Bode plot in Figure 2f,g. Impedances were highly consistent within each material group with average standard deviations of 26%, 18%, 9.4%, and 8.3% for Pt, IrOx, nanoPt, and PEDOT, respectively, when measured across a frequency spectrum from 1 Hz to 100 kHz. In principle, the average impedance would thus be a good approximation of the actual impedance of each coating material. Nevertheless, unless explicitly stated otherwise, in vitro

analysis was based on individual measurements of single electrodes, not on the average impedance of the material category.

It is generally accepted that the highest information content in neural spikes resides around the 1 kHz frequency, although also other frequencies are of interest, for instance, when measuring LFPs.[13] Based on this, both the 1 kHz and 10 Hz impedance were included in a more detailed signal analysis. At 1 kHz, the four electrode-materials spanned impedances from 2349 (±531) kOhm for Pt, 97 (±6.57) kOhm for nanoPt, 70 (±9.65) kOhm for SIROF and 37 (±2.57) kOhm for PEDOT/PSS, which also represented the lowest impedance measured (Figure 2f and Figure 3a). This order also held true for the impedance measured at the 10 Hz point with impedance magnitude being ≈2 orders higher compared to the 1 kHz data (Figure 2f and Figure 3d).

2.2. Coatings Reduce Impedance and Increase SNR

To first estimate the influence of noise, and its relation to electrode impedance in a manner completely decoupled from the biological variability, we simulated a recording by measuring the interference of ambient noise when recording a 1 kHz or 10 Hz signal, generated by a signal generator coupled over two electrode plates immersed on either side of the recording probes (Figure 2f). An SNR was calculated based on the signal intensity at the respective frequency, normed to the dominant noise contribution in the recorded signal, here the 50 Hz line noise. The expectation is that a lower impedance of the recording electrode is reflected in a higher SNR at the electrode due to larger capacitance and smaller displacement currents in capacitive interferences, as confirmed by the experimental data (Figure 3b,c,e,f). The lowest/highest impedance electrodes (PEDOT/PSS and Pt respectively) exhibited the highest/lowest SNR, both for the 1 kHz (Figure 3b) and 10 Hz (Figure 3e) signal frequency. Furthermore, the gradual decrease in impedance represented by the different materials was reflected in a corresponding gradual increase in SNR (Figure 3c,f). Although the employed materials do not allow sufficient numbers of impedance data points to statistically judge if this relation is proportional, the overall trend is clear (Figure 3c,f). The lower the impedance, the higher the SNR.

2.3. In Vitro Impedance and Not Electrode Material Determines the SNR

One of the major arguments for using high-efficiency electrode coatings is that this makes it possible to reduce electrode size without compromising recording performance. Electrode area is the major determinant of the electrode impedance.[3d] By using special probes featuring electrodes of varied sizes (Figure S3, Supporting Information), we were able to measure the recording characteristics in relation to the size of the electrode for each material, and thereby indirectly concerning to a varied impedance. The SNRs (Figure 3g,i) demonstrate the strong correlation between low impedance (here generated by the larger area) and high SNRs within each material category. Furthermore, when comparing data from the different electrode coatings, it is clearly the impedance, and not the type of electrode coating, that is the main factor determining the SNR, as they all group according to impedance rather than to material. For clarity, an overview of each individual coating is included as a supplementary figure (Figures S4 and S5, Supporting Information). From the graphs presented in Figures S4 and S5, Supporting Information showing SNR over impedance for individual materials, it is also apparent that there is a point where further lowering the impedance does not result in a further increase in the SNR for that material. Note that impedance in these experiments was varied by varying the electrode size. When plotting the same data sets as a function of radius instead of impedance (Figure 3h,j and Figures S4 and S5, Supporting Information), it can be seen that within each group (coating) the SNR increases with increasing area only up to a point after which there is no added increase in SNR by further increasing the radius. For our in vitro experiments this transition occurred for electrodes with a radius of around 110 µm for Pt, around 50 µm for nanoPt and 20–30 µm for SIROF and PEDOT. However, our in vitro experiments present a highly reduced configuration with only one, large amplitude signal source, and a homogenous medium. The method differentiates between electrodes of different impedances by estimating an SNR but, depending on the amplitude of the signal projected into the electrolyte¸ there will in each case come a point where the signal is so dominant that the noise becomes insignificantly small in comparison. The trade-off between electrode size and recording quality is far more complicated when recording from brain tissue as there are many, tightly packed signal sources that highly overlap in space and time and generate a highly complex aggregate signal. As such, we do not believe that the same saturation curve is likely to apply in vivo, as the individual amplitudes will be much smaller and the noise more substantial. Rather, our in vitro experiment mainly serves to qualitatively highlight the clear differentiation between low-impedance and high-impedance materials.

Apart from the obvious benefits of miniaturization (such as the possibility to include more recording channels and reducing the overall size of the probes), small electrodes are expected to have the additional advantage that reduced spatial averaging of the source signals may result in more distinct spikes.[14] Note that the signal from a neuron represents a highly localized perturbation of the electrical field which is different from the in vitro setup used here, where we aimed to generate a homogenous signal so that all electrodes would have the same spatial relationship to the source. Overall, our data (Figure 3g–i) show that in an in vitro experimentally simulated setting, low impedance and high SNR can be achieved both with large surface areas and with coatings, and the lowest impedances and highest SNRs were achieved with coatings on large electrodes. The benefits of small electrode contacts are expected to show primarily for in vivo settings. To analyze this would require performing similar analysis with electrodes of varied size in an actual in vivo recording experiment, which is in turn limited by that electrodes of varied size will not be possible to integrate at sufficiently high surface density for them to record the same neural signals. The chronic experiments therefore focused on varying only impedance, but not electrode size. This data set was complemented with a second chronic experiment where recordings from Pt electrodes of three different sizes were compared.

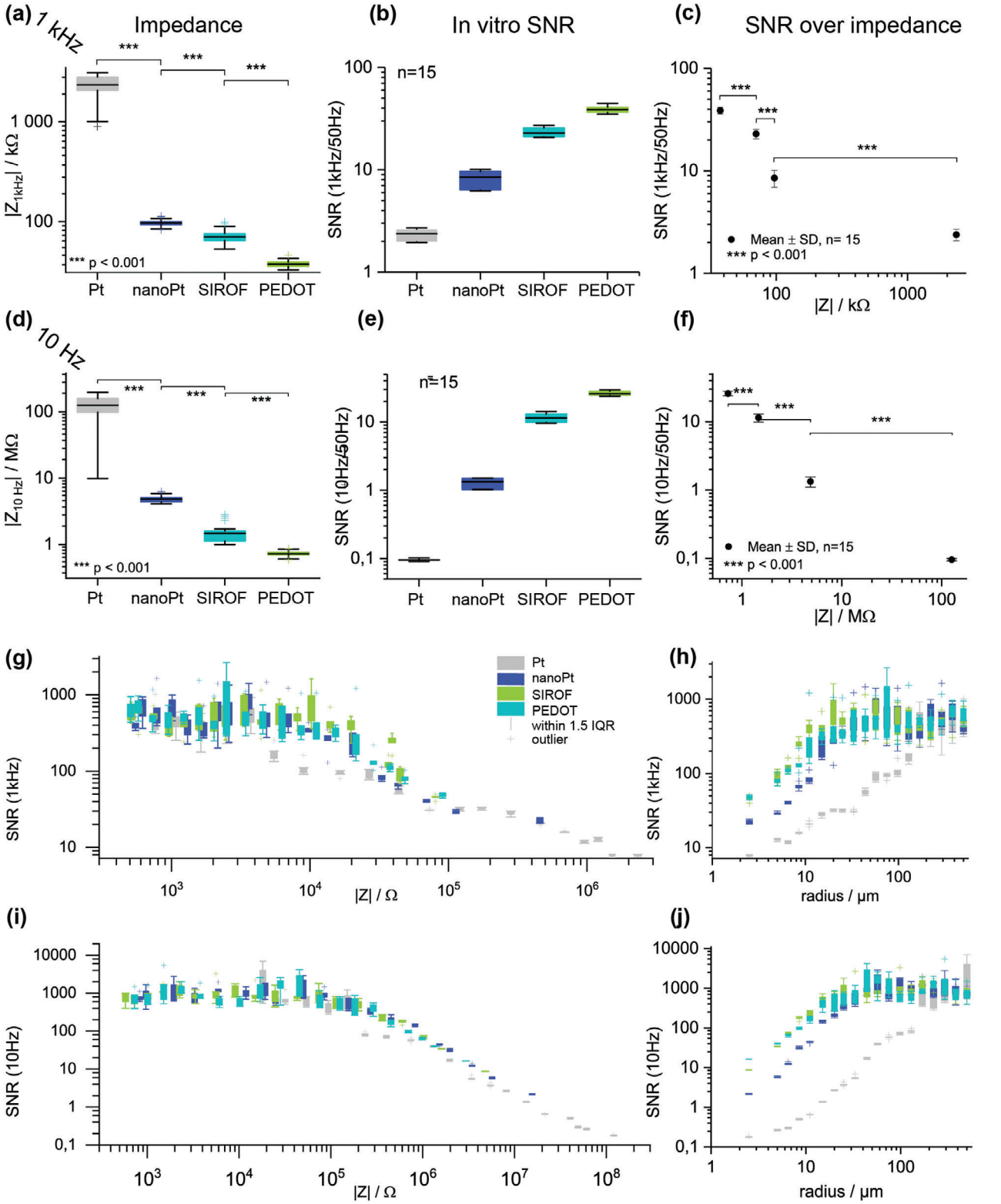

Figure 3. In vitro electrode impedance and signal-to-noise ratio characterization of 12 µm diameter electrode sites with different coatings. a) 1 kHz impedance (i.e., close up of data in Figure 2f,g) here as boxplot with different material classes on the *x*-axis ($n = 44$). For all box-plots, whiskers indicate within 1.5 IQR and line shows mean. b) SNR measured using the setup in Figure 1f for a 1 kHz signal versus 50 Hz noise. c) Same data as in (b), but here as a function of the impedance. d–f) Same as (a–c), but for 10 Hz. g) SNR-data at 1 kHz measured with the electrodes covering a range of different electrode areas (Figure S3, Supporting Information) color coded according to material and plotted as a function of impedance and in (h) as a function of electrode radius. i,j) Same as (g,h), but for 10 Hz.

2.4. Chronic Recording Quality with Low Impedance Coatings

To evaluate the effect of surface coating and electrode impedance on the quality of extracellular electrical activity recorded in vivo, we implanted arrays into the dorsal hippocampus (CA1) of wild-type mice (C57BL/6). We were able to record extracellular voltages from all electrodes within 2 days of implantation, and arrays were stable for an average of 11 weeks (minimum 6 weeks). Signal quality and impedances were highly stable across the period of implantation (**Figure 4**), and multi-unit and single-unit activity was observed on all electrode types. While we observed detectable spiking activity and were able to isolate single units on all electrode types, the coated electrode contacts recorded units with larger amplitude in general, as can be seen from the raw and high-pass filtered voltage traces (Figure 4a). Impedance was stable across the experiment in chronically implanted arrays for all electrode types (Figure 4b). Surprisingly, the difference of impedance after implantation (the change in impedance measured just prior to implantation in vitro and one week post-implantation in vivo) was not the same for all electrode treatments, but high-impedance electrodes exhibited a proportionally higher offset (Figure S6, Supporting Information).

Subsequently, we investigated the amplitude of detected single units by electrode type. As expected, we found that all coated electrodes had larger amplitudes than the untreated platinum electrodes, with the PEDOT coating having the overall largest amplitudes. Individual examples of representative units detected on each electrode type are shown in **Figure 5**a–d, which depicts units detected at one of each electrode type, and the spike-triggered average across the array. The ability to isolate single units also varied not only with electrode impedance, but also with electrode size. We found that large Pt electrodes (0.1 mm × 0.5 mm sites) recorded high SNR low-frequency activity, but the large size led to spatial blurring and reduced high-frequency SNR that obscured the single units and prevented spike sorting (**Figure 6**a). Reducing the size of Pt electrodes (0.03 mm diameter) improves high frequency SNR, enabling the identification of single units (Figure 6b). Electrode size and coating minimally changed the power spectral density of the broadband voltage recorded in vivo, and all electrodes had qualitatively similar power distributions (Figure S7, Supporting Information). Ultimately, high-density arrays with many contacts further improve single unit isolation and increase spatial resolution. However, further reducing the size of Pt electrodes (12 µm diameter) reduces their SNR and again prevents the reliable isolation of single-units (Figure 6c). As previously demonstrated, coating electrodes lowers their impedances and improves their high frequency SNR. Across the three coatings used in this study, we found that unit isolation quality and yield improved with lower impedance (Figure 6d–f). The population data across electrode coatings and size reveals that reducing electrode size and lowering impedance improve the SNR and isolation of recorded units. Coated electrodes of a given size record single-unit activity with a higher SNR, having larger spike amplitude and higher average per electrode unit-yield than untreated platinum electrodes (summarized in **Figure 7**a,b). It is possible that unit yield and SNR would further improve for even smaller electrode contacts if impedance was held constant or further reduced. Indeed, for high-density multi-electrode arrays developed for in vitro applications, electrodes with half the surface area compared to those in the present study are able to record high-SNR action potentials.[15] Further studies are necessary to determine if there is an optimal size for coated electrodes of a given impedance to record high-SNR unit activity in vivo, or if smaller always is better.

Finally, we investigated the presence of movement artifacts in awake, mobile mice as a function of electrode type. We found that during periods of movement, the untreated platinum electrode contacts experienced increased amplitude movement artifacts due to capacitive coupling compared to treated electrodes (**Figure 8**). The magnitude of the movement artifact varies depending on the degree of movement of the animal but was isolated to platinum electrodes. The artifact was dominated by low frequencies and did not affect the isolation of single units in the recordings; however, it complicates the analysis of the local field potential in awake behaving animals.

3. Discussion

We fabricated flexible, multi-electrode arrays featuring densely spaced electrode sites with four different surface treatments. The materials were selected to provide a range of impedances from high to low, for the same shape and geometrical area of the electrodes. The primary point of the study was to investigate if impedance matters for recording quality. We first investigated this question using a non-biological model, with signals generated over two electrode plates immersed in an electrolyte and with the recording electrode placed at the center, in a similar arrangement as described by Nelson et al.[6a] Impedance spectroscopy drives a known current (or voltage) across an electrode at a range of frequencies, while measuring the corresponding voltage necessary (or the resulting current) to achieve the target. To estimate the SNR of our electrodes, we constructed the inverse experiment, a setup with a known alternating voltage at a frequency of interest in the solution, and measured the fidelity with which the electrode could record the signal. The results clearly demonstrate that electrode impedance is negatively correlated to the signal-to-noise ratio, that is, electrodes with lower impedance have a larger SNR, both at the lower (10 Hz) and higher (1 kHz) frequency tested (Figure 3c,f). We then added a similar measurement, using probes that featured electrodes of the same material, but of variable radius. The experiment was repeated for all materials in our study. The result once more confirmed that under these conditions, the primary electrode property determining the SNR is the impedance of the electrode. Larger electrodes displayed higher SNR, because of their lower impedance (Figure 3g–j). In other words, in the in vitro experiment it did not matter for the SNR if the electrode had low impedance due to its large area or because of a more efficient material. A saturation effect was also seen where lowering impedance/increasing the area below/above a certain point did not further increase the SNR. It should be noted that this is different from the in vivo measurement where the signal source is much weaker and furthermore localized to a specific point of similar geometric scale as the area of the electrodes.

Second, we investigated the same question with the probes chronically implanted in the mouse hippocampus to record in vivo for up to 12 weeks. The ability of a single electrode to detect a unit will, apart from the properties of the electrode itself, depend on the distance between the source and the electrode,

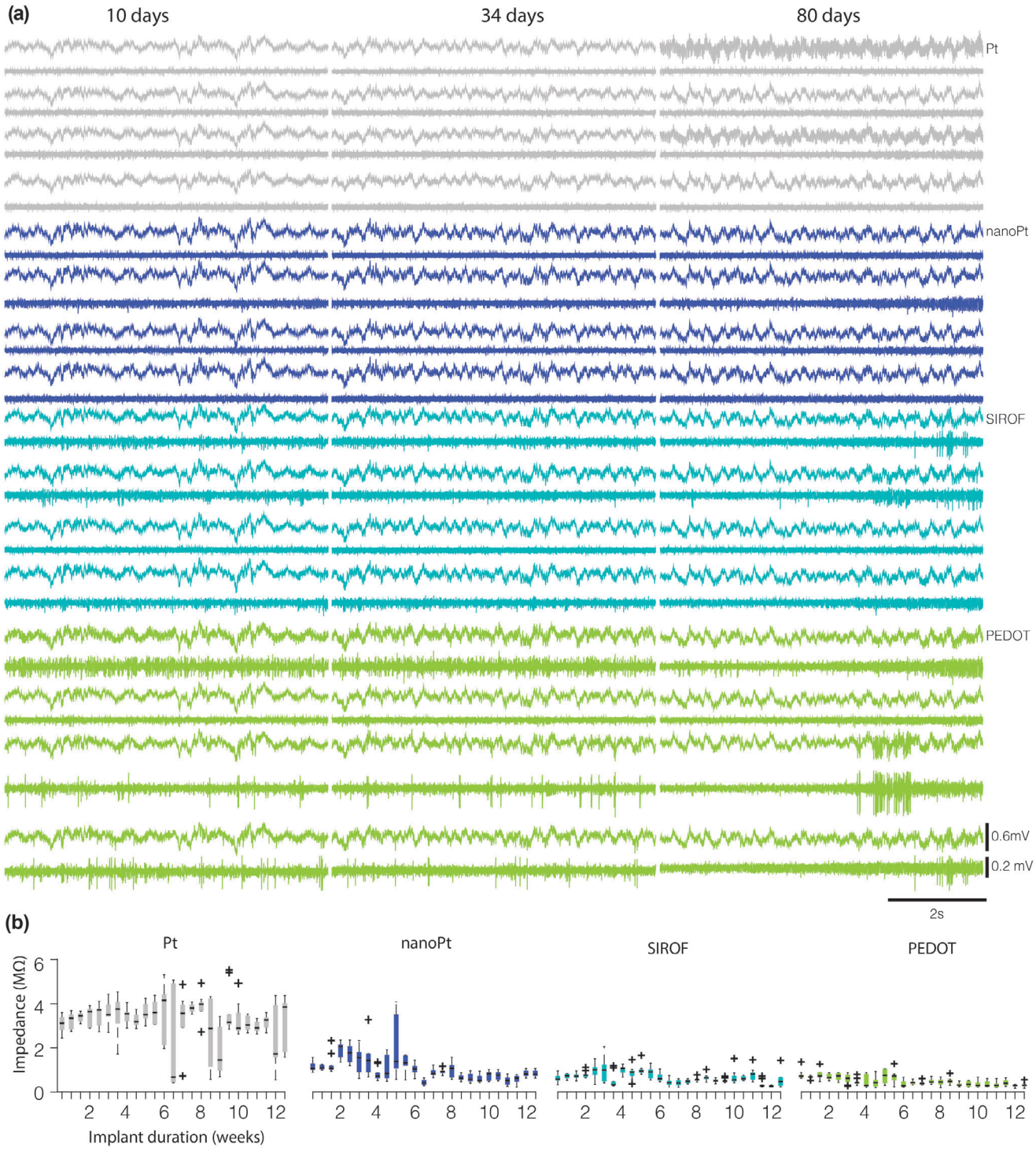

Figure 4. In vivo recording quality and impedance stability for 12 µm diameter electrode sites across coatings. a) Data from one chronically implanted array. Electrodes are sorted by contact type, columns show example traces at 10 days (left), 34 days (middle), and 90 days (right) post implant. Two signals are shown for each electrode the broadband signal (top) and the highpass signal (480 Hz, bottom). The scales for broadband and highpass are different, but are kept the same across all electrodes. b) Longitudinal impedance data for all electrode types measured for the length of the chronic implantation up to 12 weeks.

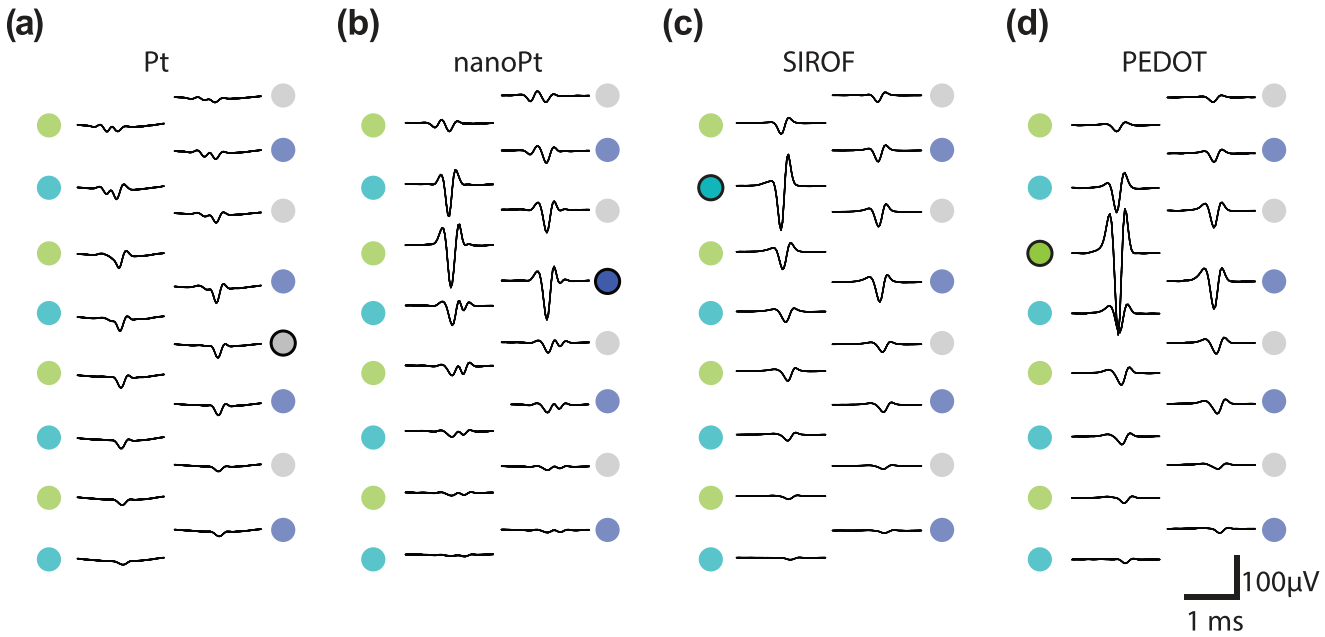

Figure 5. In vivo single-unit separation and amplitude for 12 μm diameter electrode sites across coatings. a) Example unit detected on a platinum electrode (12 μm diameter). The unit was detected based on threshold-crossing of the high-pass voltage (480 Hz) on the indicated electrode site (black outline around electrode indicates the site were the unit was detected). The waveform of the simultaneous voltage is displayed across the array, demonstrating variation in the unit amplitude for the same unit recorded at different spatial positions with different electrode coatings. Time and voltage scale are the same for (b–d) as shown in panel (d). b) Same as panel (a) but for a unit detected on nanoPt electrode. c) Same as panel (a) but for a unit detected on SIROF electrode. d) Same as panel (a) but for a unit detected on PEDOT electrode.

and the resistive qualities of the biological media between the two.[16] These aspects were considered in two ways in the probe design. By using a thin-film flexible probe, encapsulation from glial scarring was reduced as has been previously demonstrated in several earlier studies.[4a,11,17] Reduced scarring makes it more likely to record spikes throughout the test period of 12 weeks. Limiting the entire electrode-covered section of the probe to an area less than 400 μm long and 60 μm wide, increased the likelihood that even in the presence of gliotic scarring, the reaction was similar throughout the entire electrode-covered portion. Furthermore, keeping electrodes densely spaced (45 μm pitch) makes it likely that a spike seen on one electrode is visible on several other nearby electrodes simultaneously. Low- and high-impedance electrodes would thereby occasionally record the same spike, and experience overall comparable signaling and scarring environment.

The chronic recording data collected underscores the main point that low impedance is essential for increasing the quality of electrophysiological recordings. Low-impedance electrodes had higher average unit yield, and furthermore, higher unit amplitudes were measured on low impedance electrodes, compared to those with high impedance. PEDOT-coated electrodes, which had the lowest impedance, also had the highest unit yield and recorded units with larger amplitude, followed by SIROF, nanoPt and Pt electrodes, in that order, and in order of increasing impedance. This verifies the view that the recording electrode and amplifier forms a voltage-divider circuit attenuating the amplitude of the signal.[5] Furthermore, high-impedance electrodes exhibited the largest motion artifacts, which can limit the analysis of local field potential during awake recordings.

All of the above is not unexpected, but rather experimentally settles a discussion point which has been open for some time. To selectively study single spikes, electrodes need to be small enough to distinguish spatially inter-mingled neurons. Applying surface coatings to an electrode of a given size increases the effective surface area of the electrode and improves transduction of the neural signals, improving SNR, spike detection, and spike isolation, in result this increases the unit-yield for a given electrode. That is the main conclusion of our study. Signal quality and unit yield are negatively correlated with electrode impedance. While classical methods of electrode fabrication did not allow to accomplish reduced electrode size without increasing impedance, modern materials allow to counteract the impedance increase. Thus, unit recordings are enabled by the small electrode size simultaneously as high SNR is enabled by the reduced impedance, which together allow recording of spatially-defined biopotentials.

It is worth noting that a paper by Neto et al. published in 2018 came to the opposite conclusion, namely that impedance did not affect the quality of their recordings.[8] Some essential differences between our study and the Neto study may explain this inconsistency. First, Neto et al. performed acute recordings in anesthetized animals, while our study focused on chronic recordings in awake animals collected over months. In the case of acute electrode insertion, it is likely that the probe tissue interface is quite different from that during chronic implantation, when the tissue has adapted to the presence of the probe. For instance, swelling in the acute phase may impact the probe-tissue contact and press signal sources closer to the electrode surface in the Neto study, which could reduce the effect of impedance as the neuron–electrode coupling will be different if there is direct

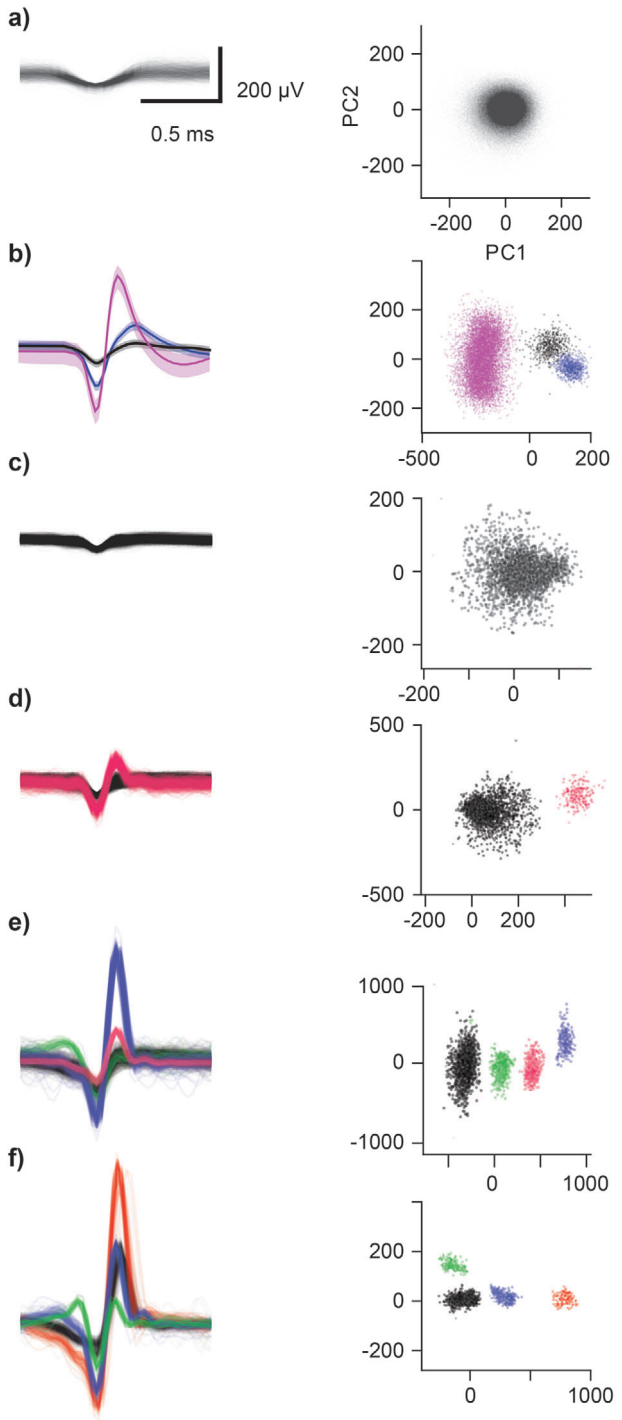

Figure 6. In vivo single unit detection depends on electrode size and impedance. a) Example multi-unit recorded with a large platinum intracortical electrode (0.1 mm × 0.5 mm). Left, overlap of individual threshold-crossings of the high-frequency bandpass signal showing low-amplitude and undifferentiated waveforms. Right, low dimensional projection of the first two principal component dimensions for the waveform shape showing one broad cluster of individual threshold events. Large sites can record high SNR LFP but are not able to isolate single units and record a mixture of many units. b) Example of single units recorded with a platinum intracortical electrode of intermediate area (30 µm diameter). Intermediate electrodes are able to distinguish multiple single units. c) Example multi-unit recorded with a small platinum electrode (12 µm diameter). Small platinum electrodes have a high impedance and cannot reliably distinguish single units. d) Example single unit recorded with a nanoPt coated electrode (12 µm diameter). Coating reduces the impedance and increases the identification of single units. e) Example single units recorded with an IrOx coated electrode (12 µm diameter). Coating further reduces the impedance and increases the SNR with which single units can be identified. f) Example single units recorded with a PEDOT coated electrode (12 µm diameter). Coating reduces the impedance and increases the identification of single units.

contact between the two. Brain tissue in physical contact with the electrode surface is notably different as compared to a defined gap of electrolyte separating the tissue and electrode.[5] Likewise, under anesthesia, the brain is in a very different dynamical state; as compared to the awake state; under anesthesia, neurons have overall lower firing rates, far less background activity, and neurons often spike in bursts of activity that are synchronized across large populations of neurons. However, based on our data, we feel confident to say that decreasing impedance improves SNR, unit amplitude and unit yield per electrode. While impedance is important, other aspects, both surgical and technological, must be optimized to get the best possible data quality. Surgically, recording quality can be improved by several factors, such as slow insertion, minimizing bleeding and minimizing the dimpling of the tissue upon insertion.[18] Technologically, other factors such as the headstage and amplifier, as well as the overall probe design and insertion, should be optimized to improve minimal distortion and the highest fidelity recording of signals of interest.[5,6,19]

The materials included in our study were selected to cover different aspects of electrode surface qualities to evaluate if material properties beyond impedance matter for recording quality. All the materials included have previously been demonstrated as suitable electrode materials for in vivo use with sufficient bio-compatibility. The closest comparison is between Pt and nanoPt, since the latter only adds nano-porosity to manipulate the impedance, while the material itself is the same. The porous nature of SIROF electrodes adds roughening as well as a valence change oxide system, where the latter could provide additional charge transfer reactions to further lower the charge-transfer resistance.[3d] The hydrophilic nature of PEDOT-coatings as well as their hybrid electron–ion charge transfer properties, are often mentioned as arguments for why these would perform particularly well in neural recordings.[7a,10b,c] The secondary aim of this study was to also analyze if these additional qualities substantially added to improved recording quality, beyond the low impedance. From our data, we did not see any such additional materials-specific benefits, but rather that recording quality closely follows the impedance characteristics. More subtle effects could of course still be present, but based on our data we do not see that a substantial additional contribution could be expected other than impedance. Worth noting is that recording quality should not be confused with the desirable properties for electrical stimulation, where such materials-specific qualities are essential for safe charge injection.

Last, but not least, we would like to highlight some additional aspects of our study that contribute other than the points

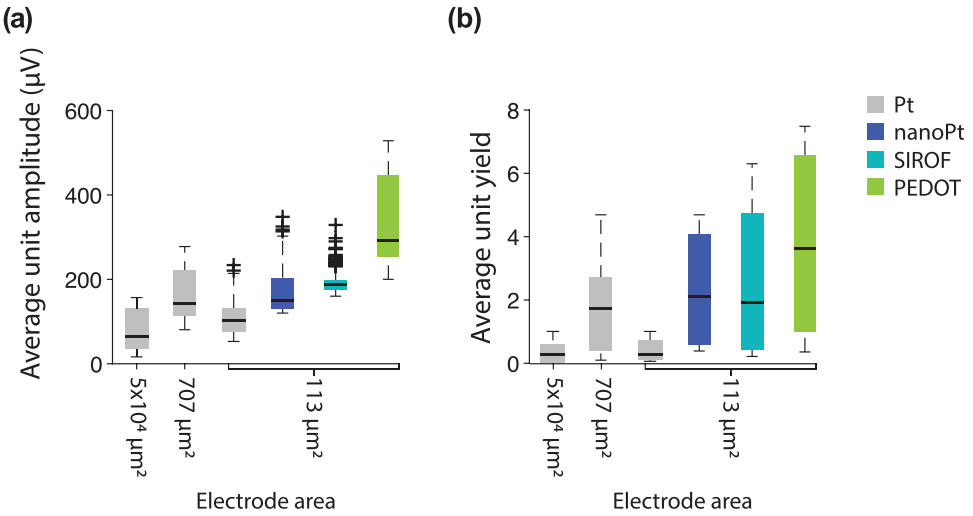

Figure 7. In vivo single-unit amplitude and yield for different electrode sizes and coatings. a) Average unit amplitude (the peak-to-peak magnitdue ± 0.5 ms around threshold crossing) across the population of units detected for each electrode type. The size of the electrode is indicated on the x-axis and the coating for 12 μm diameter electrodes is indicated by the bar color. b) Average number of single units recorded per electrode across the population of units detected for each electrode type.

related to impedance and recording quality. Compared to recent work on high-density flexible intracortical arrays, the arrays presented here are designed to be much wider than what would be ideal to reduce glial scarring in the longer term.[3a,11] Despite this, our electrode achieved long-term chronic recordings in vivo over 12 weeks. The dense distribution of electrodes on the active part of the arrays enabled the spatial signature of individual units to be discriminated, attesting to the overall high quality of the recordings made and the stability of the probe over time. In vivo measured electrode impedances were stable across the duration of the implant, and followed the internal relation seen between the materials when measured in vitro. In vitro and in vivo measured impedance was also compared across probes and materials, this time using the same device to measure impedance in both environments (2-electrode configuration) and considering only the 1 kHz impedance point. When we measured the impedance of the same electrodes in vitro prior to implantation and in vivo after implantation, the impedance increased, as expected. Brain tissue has a higher impedance than saline and thus, the resulting electrode–tissue interface has higher impedance than the electrode–saline interface. Given that the electrodes are closely spaced, one could have expected this added load to be largely the same across all electrodes. However, the difference in pre-implant in vitro impedance and post-implant in vivo impedance was not a fixed contribution identical across all electrode types, but high-impedance electrodes had a larger increase in impedance after implantation as compared to low-impedance electrodes (Figure S6, Supporting Information). It is possible that this impedance-dependent change in electrode-tissue coupling depends on the precise electrolytic interface between the electrode and the tissue and could reflect other aspects of the impedance, such as additional capacitances and the number of possible ion exchanges between the electrolytes in brain tissue and the electrode-coating. The "real" (electrochemical) surface area is larger in rough electrodes (nanoPt), valence change materials (SIROF) and volume conductivity materials (PEDOT) compared to their geometrical surface area as the impedance spectra (Figure 2f,g) indicate: Therefore, different in vivo access resistances might occur that lead to this increased impedances. This point would be interesting to investigate further in future work, especially to derive design rules to predict in vivo impedance of electrodes based on in vitro data.

Overall, we find that recording quality is systematically related to electrode impedance, as would be expected from theory, and as such, continued development of methods to reduce the impedance of miniaturized electrodes is fully justified to improve the fidelity of brain computer interfaces for basic science, as well as for clinical applications.

4. Experimental Section

Probe Fabrication: Flexible polyimide probes were fabricated following standard MEMS cleanroom fabrication protocols as previously described in Boehler et al.[3a,17] In brief, a 5 μm thin polyimide layer (U-Varnish S, UBE) was spin-coated onto a silicon wafer and subsequently imidized at 450 °C in a vacuum oven. After O_2-plasma activation (30 s at 100 W), a 300 nm thin platinum layer was sputtered onto the polyimide and photolithographically patterned to define the electrode sites and interconnection tracks. Iridium oxide was subsequently sputtered to a thickness of 800 nm on a subset of the electrode sites using a second photolithographic patterning step. The metal tracks were finally insulated with a second layer of polyimide (5 μm), which was patterned via reactive ion etching in an O_2-plasma to define the electrode sites as well as the overall contour of the polyimide probe as shown in Figure 2. The resulting probe provides 17 individual electrode sites with a diameter of 12 μm placed at a pitch of 45 μm along the shaft. A hole is integrated at the tip of the probe to facilitate implantation using a shuttle engaged with the hole (Figure 2d,e). To investigate the effect of electrode size on SNR and single unit recording arrays with varying sized, uncoated-electrode contacts (platinum electrodes embedded in polyimide) were fabricated in the same manner.

Electrode Materials: Four different electrode coatings were realized on each polyimide probe in an alternating pattern as shown in Figure 2, to allow for simultaneous recordings with multiple electrode materials of

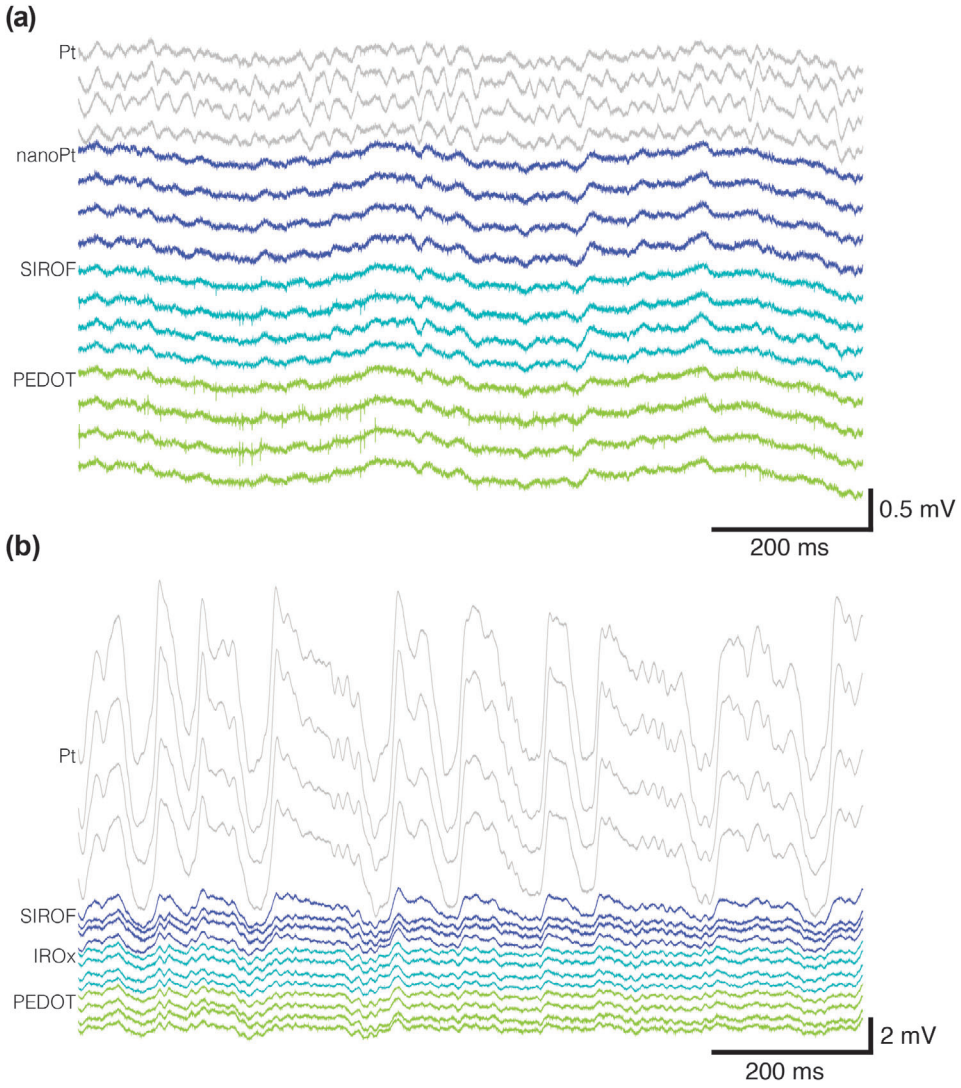

Figure 8. Low frequency movement artifacts dominate recording on uncoated electrodes. During recordings in awake animals, movements contaminate high-impedance electrodes. a) Example session with minor movement artifacts. Artifacts are low frequency alterations in the voltage apparent on the platinum electrodes, but much diminished or invisible on the low impedance electrodes. b) Example session with bad movement artifacts. Movement of the animal leads to large variations in voltage on the platinum electrodes and to a lesser degree on low impedance coated electrodes. All electrodes were 12 µm diameter.

different impedance from the same implant. The distribution of the electrode materials on the probe shank is available in Figure S2, Supporting Information. Smooth platinum and SIROF were readily available after cleanroom fabrication on half of the electrode sites, respectively. The conducting polymer PEDOT/PSS was deposited on a subset of the SIROF coated electrode sites by means of an electrochemical polymerization process as described in Boehler et al.[12] A charge density of 200 mC cm^{-2} was employed during the potentiostatic polymerization, conducted at 0.9 V versus Ag/AgCl in an aqueous electrolyte containing ethylene dioxythiophene (EDOT) and sodium-polystyrenesulfonate (NaPSS) at a concentration of 0.01 M and 5 mg mL^{-1}, respectively, to reach a PEDOT coating thickness of ≈1 µm. The nanostructured platinum coating (nanoPt) was electrochemically deposited onto half of the platinum sites following the deposition protocol described in Boehler et al.[9b] The implant was immersed into an electrolyte containing 2.5 mM H_2PtCl_6, where a potential of −0.2 V versus Ag/AgCl was applied to selectively deposit nanoPt onto the electrode sites resulting in growth of a 3D Pt structure as shown in Figure 2c. Deposition was here performed with a charge density of 7 nC $µm^{-2}$, resulting in a grass morphology with feature sizes in the order of ≈1 µm in height.

In Vitro Characterization: After fabrication, all probes were electrochemically characterized in vitro to benchmark the performance of the individual electrode materials. These measurements were performed according to the guidelines for electrode characterization described in Boehler et al.[3d] Impedance values for different frequencies were extracted from electrochemical impedance spectroscopy measurements, which were realized in phosphate buffered saline (PBS, 0.01 M) using sinusoidal excitation signals with amplitudes of 100 mV_{PP}. Next to the entire frequency spectrum (measured from 0.1 Hz to 100 kHz) and evaluation of the cutoff-frequency, particular focus was set to the impedance at a frequency of 10 Hz, representing the average frequency domain associated with local field potential (LFP) recordings, as well as a frequency of 1 kHz, representing the frequency domain relevant to single/multi-unit activity (SUA/MUA) recordings. These measurements were all collected using the Metrohm AUTOLAB PGSTAT system, depending on daily access the PGSTAT 128, 204, or 302 model from this manufacturer.

SNR measurements were performed using the setup shown in Figure 2h. Sinusoidal signals at different frequencies (10 Hz and 1 kHz) with an amplitude of 100 mV_{pp} were applied between two stainless steel electrodes (area: 4 cm^2) immersed in PBS (0.01 M). A probe placed in the center of the 70 × 30 × 20 mm^3 large beaker was used to record the injected signals across all electrode materials using an oscilloscope. These signals were analyzed by fast Fourier transformation (FFT) and the SNR subsequently calculated from the signal intensity at the target frequency normed to the dominant noise contribution in the recorded signal, which was here the 50 Hz line noise.

Implantation and In Vivo Measurements: All experimental procedures were carried out in accordance with the guidelines of the Federal Veterinary Office of Switzerland and were approved by the Cantonal Veterinary Office in Zurich under license number 153/2019.

Chronic electrophysiological recordings were performed in eight wild-type (black-6) male mice. Implantation targeted the CA1 subfield of the dorsal hippocampus. During implantation, animals were anesthetized with isoflurane (2–4% for induction, 1–2% during surgery) and their body temperature was maintained using a heating pad. The scalp was retracted, and the skull was exposed and sealed with dental acrylic. A small craniotomy was performed and the probe was inserted into the brain by coupling with a steel insertion needle.[20] Two additional trepanations were performed over the cerebellum and the frontal cortex, and a silver wire was placed in contact with the CSF to serve as ground and reference electrodes. After implantation the probe was fixed in place with additional acrylic and the connector was affixed to the animal's head. The animal was allowed to recover for 2–4 days after the surgery and then recording proceeded on a regular basis. Recording was performed either during anesthesia, or while the mouse was awake. For anesthesia recordings, the animal was anesthetized with isoflurane (2–4% for induction, 0.5–1% during recording) and their body temperature was maintained using a heating pad. During awake recordings, the animal was placed in an enclosed, sound-proof box and head-fixed. For electrophysiological recording, the voltage was amplified and digitally sampled at a rate of 30 kHz using a commercial extracellular recording system (Intan). The raw voltage traces were filtered off-line to separate the multiunit activity (MUA) (highpass filter frequency of 480 Hz) using a second-order Butterworth filter. Subsequently, for each electrode, a threshold was applied to the highpass filtered data to isolate multi-units and reject background noise (5 times the standard deviation across the recording session, specified per electrode). The SNR was computed as a ratio of the peak voltage exceeding the 5-STD threshold and the RMS of the signal.

Statistical Analysis: For electrochemical and in vitro test data, impedance spectroscopy and SNR data was collected in 44 replicates (electrode sites) per material (n = 44) distributed over 11 probes. Impedance data for each frequency point was reported as the average of those 44 measurements at that point, with whiskers representing standard deviation over the 44 measurements for that material and frequency (Figure 2). SNRs where collected for the same set of electrodes (n = 44) and each data point was reported with a box-and-whiskers plot (Figure 3) where the box represents the 25–75% and the whiskers note the 1.5 interquartile range (IQR). Outliers are reported as specified in the graphics. In vivo electrode measurements were made using 8 probes in 8 mice. Each array contained 4 sites of each recording type, giving a total of 32 electrode sites for each surface treatment. In vivo impedance data reported in Figure 4b and Figure S6b, Supporting Information indicate the average for all electrode sites of each surface coating at each time point and whiskers indicate standard deviation over the 32 measurements for that material. Average unit amplitude and yield reported in Figure 7 are likewise aggregated across all electrode sites of each type and box plot indicates the mean and standard deviation.

Supporting Information

Supporting Information is available from the Wiley Online Library or from the author.

Acknowledgements

C.M.L. thanks Fritjof Helmchen for infrastructure and funding support for a portion of the experiments reported in this manuscript. This work was supported by a Forschungskredit from the University of Zurich (project K-41220-04, C.M.L.). C.B., M.A., and T.S were supported by BrainLinks-BrainTools, Cluster of Excellence funded by the German Research Foundation (DFG, EXC 1086), currently funded by the Federal Ministry of Economics, Science and Arts of Baden Württemberg within the sustainability program for projects of the excellence initiative. MA. and C.B. furthermore were supported by the European Union's Horizon 2020 Research and Innovation Program (Grant Agreement No. 899 287 NeuraViPeR).

Conflict of Interest

P.F. and C.M.L. have a patent on thin-film electrodes. P.F. is member of the Advisory Board of CorTec GmbH (Freiburg, Germany).

Author Contributions

C.M.L., C.B., R.L., T.S., and M.A. designed research; C.B. and R.L. fabricated arrays and performed in vitro evaluation, C.M.L. performed in vivo experiments and analyzed data, C.M.L., C.B., and M.A. wrote the paper. All authors gave feedback and revised the manuscript.

Data Availability Statement

The data that support the findings of this study are available from the corresponding author upon reasonable request.

Keywords

bioelectronics, electrochemical impedance spectroscopy, electrophysiology, flexible probes, microelectrodes, neural probes, neurotechnology

Received: October 6, 2023
Revised: January 19, 2024
Published online:

[1] a) D. H. Hubel, *Science* **1957**, *125*, 549; b) G. E. Loeb, R. A. Peck, J. Martyniuk, *J. Neurosci. Methods* **1995**, *63*, 175.

[2] a) G. Buzsáki, *Nat. Neurosci.* **2004**, *7*, 446; b) C. M. Gray, P. E. Maldonado, M. Wilson, B. McNaughton, *J. Neurosci. Methods* **1995**, *63*, 43; c) J. J. Jun, N. A. Steinmetz, J. H. Siegle, D. J. Denman, M. Bauza, B. Barbarits, A. K. Lee, C. A. Anastassiou, A. Andrei, Ç. Aydın, M. Barbic, T. J. Blanche, V. Bonin, J. Couto, B. Dutta, S. L. Gratiy, D. A. Gutnisky, M. Häusser, B. Karsh, P. Ledochowitsch, C. M. Lopez, C. Mitelut, S. Musa, M. Okun, M. Pachitariu, J. Putzeys, P. D. Rich, C. Rossant, W. L. Sun, K. Svoboda, et al., *Nature* **2017**, *551*, 232; d) C. M. Lewis, C. A. Bosman, P. Fries, *Curr. Opin. Neurobiol.* **2015**, *32*, 68; e) B. L. McNaughton, C. A. Barnes, J. O'Keefe, *Exp. Brain Res.* **1983**, *52*, 41.

[3] a) C. Böhler, M. Vomero, M. Soula, M. Vöröslakos, M. Porto Cruz, R. Liljemalm, G. Buzsaki, T. Stieglitz, M. Asplund, *Adv. Sci.* **2023**, *10*, 2207576; b) D. R. Humphrey, E. M. Schmidt, in *Neurophysiological Techniques. Neuromethodsm* (Eds: A. A. Boulton, G. B. Baker, C. H. Vanderwolf), Vol. *15*, Humana Press, **1990**; c) L. Klein, F. Pothof, B. C. Raducanu, J. Klon-Lipok, K. A. Shapcott, S. Musa, A. Andrei, A. A. Aarts, O. Paul, W. Singer, P. Ruther, *J. Neural Eng.* **2020**, *17*, 026036; d) C. Boehler, S. Carli, L. Fadiga, T. Stieglitz, M. Asplund, *Nat. Protoc.* **2020**, *15*, 3557.

[4] a) C. Xie, J. Liu, T.-M. Fu, X. Dai, W. Zhou, C. M. Lieber, *Nat. Mater.* **2015**, *14*, 1286; b) S. Zhao, X. Tang, W. Tian, S. Partarrieu, R. Liu, H. Shen, J. Lee, S. Guo, Z. Lin, J. Liu, *Nat. Neurosci.* **2023**, *26*, 696; c) Z. Zhao, H. Zhu, X. Li, L. Sun, F. He, J. E. Chung, D. F. Liu, L. Frank, L. Luan, C. Xie, *Nat. Biomed. Eng.* **2023**, *7*, 520.
[5] L. Guo, *J. Neural Eng.* **2020**, *17*, 013001.
[6] a) M. J. Nelson, P. Pouget, E. A. Nilsen, C. D. Patten, J. D. Schall, *J. Neurosci. Methods* **2008**, *169*, 141; b) R. Quian Quiroga, S. Panzeri, *Nat. Rev. Neurosci.* **2009**, *10*, 173.
[7] a) R. Green, M. R. Abidian, *Adv. Mater.* **2015**, *27*, 7620; b) P. Yin, Y. Liu, L. Xiao, C. Zhang, *Polymers* **2021**, *13*, 2834; c) S. F. Cogan, T. D. Plante, J. Ehrlich, *The 26th Ann. Int. Conf. of the IEEE Engineering in Medicine and Biology Society*, IEEE, San Francisco, CA, 2004, p. 4153.
[8] J. P. Neto, P. Baião, G. Lopes, J. Frazão, J. Nogueira, E. Fortunato, P. Barquinha, A. R. Kampff, *Front. Neurosci.* **2018**, *12*, 00715.
[9] a) C. Boehler, T. Stieglitz, M. Asplund, *Biomaterials* **2015**, *67*, 346; b) C. Boehler, D. M. Vieira, U. Egert, M. Asplund, *ACS Appl. Mater. Interfaces* **2020**, *12*, 14855.
[10] a) G. E. Fenoy, O. Azzaroni, W. Knoll, W. A. Marmisollé, *Chemosensors* **2021**, *9*, 212; b) Y. Liang, A. Offenhäusser, S. Ingebrandt, D. Mayer, *Adv. Healthcare Mater.* **2021**, *10*, 2100061; c) T. Araki, L. M. Bongartz, T. Kaiju, A. Takemoto, S. Tsuruta, T. Uemura, T. Sekitani, *Flexible Printed Electron.* **2020**, *5*, 043002.
[11] a) J. E. Chung, H. R. Joo, J. L. Fan, D. F. Liu, A. H. Barnett, S. Chen, C. Geaghan-Breiner, M. P. Karlsson, M. Karlsson, K. Y. Lee, H. Liang, J. F. Magland, J. A. Pebbles, A. C. Tooker, L. F. Greengard, V. M. Tolosa, L. M. Frank, *Neuron* **2019**, *101*, 21; b) L. Luan, X. Wei, Z. Zhao, J. J. Siegel, O. Potnis, C. A. Tuppen, S. Lin, S. Kazmi, R. A. Fowler, S. Holloway, A. K. Dunn, R. A. Chitwood, C. Xie, *Sci. Adv.* **2017**, *3*, 1601966.
[12] C. Boehler, F. Oberueber, S. Schlabach, T. Stieglitz, M. Asplund, *ACS Appl. Mater. Interfaces* **2017**, *9*, 189.
[13] B. O. Watson, M. Ding, G. Buzsáki, *Eur. J. Neurosci.* **2018**, *48*, 2482.
[14] V. Viswam, M. E. J. Obien, F. Franke, U. Frey, A. Hierlemann, *Front. Neurosci.* **2019**, *13*, 00385.
[15] J. Müller, M. Ballini, P. Livi, Y. Chen, M. Radivojevic, A. Shadmani, V. Viswam, I. L. Jones, M. Fiscella, R. Diggelmann, A. Stettler, U. Frey, D. J. Bakkum, A. Hierlemann, *Lab Chip* **2015**, *15*, 2767.
[16] a) D. A. Henze, Z. Borhegyi, J. Csicsvari, A. Mamiya, K. D. Harris, G. Buzsáki, *J. Neurophysiol.* **2000**, *84*, 390; b) N. K. Logothetis, C. Kayser, A. Oeltermann, *Neuron* **2007**, *55*, 809.
[17] C. Boehler, C. Kleber, N. Martini, Y. Xie, I. Dryg, T. Stieglitz, U. G. Hofmann, M. Asplund, *Biomaterials* **2017**, *129*, 176.
[18] a) R. Fiáth, B. C. Raducanu, S. Musa, A. Andrei, C. M. Lopez, M. Welkenhuysen, P. Ruther, A. Aarts, I. Ulbert, *J. Neurosci. Methods* **2019**, *316*, 58; b) B. Thielen, E. Meng, *J. Neural Eng.* **2021**, *18*, 041003.
[19] R. R. Harrison, *Proc. IEEE* **2008**, *96*, 1203.
[20] a) P. Fries, C. Lewis, US Patent 11, 141, 112 **2021**; b) B. Rubehn, C. Lewis, P. Fries, T. Stieglitz, in *Proc. 15th Annu. Conf. of the IFESS*, Vienna, **2010**.